

Supporting Information

Developing a MXene quantum dots-based separator for Li-S batteries

Ke Yang, Chan Li, Haoyuan Qi, Yunfei Dai, Yuhong Cui, Yibo He*

State Key Laboratory of Solidification Processing, Center of Advanced Lubrication and
Seal Materials, School of Materials Science and Engineering, Northwestern
Polytechnical University, Xi'an, Shaanxi, 710072 P. R. China.

* Corresponding author: Northwestern Polytechnical University, Xi'an, Shaanxi, 710072 P. R. China.
Email: heyibo@nwpu.edu.cn

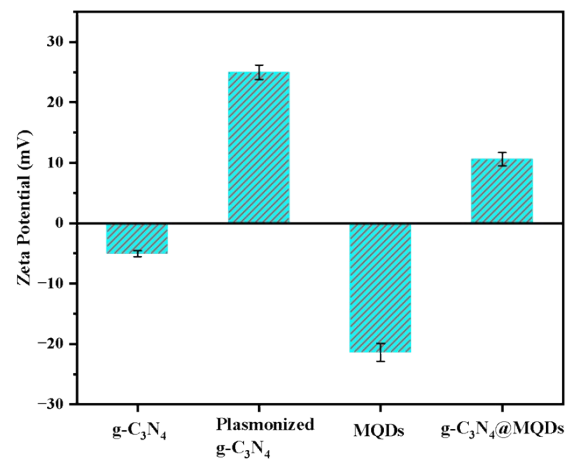


Figure S1 Zeta Potential of the obtained samples before and after compounding.

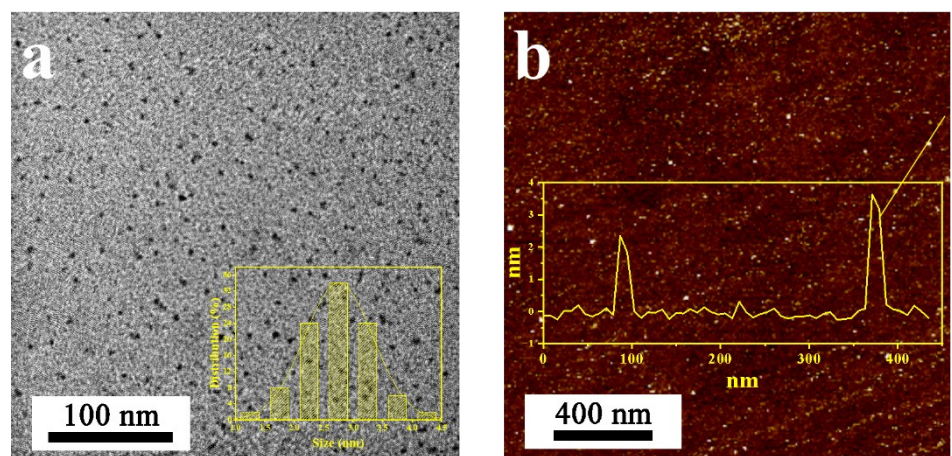


Figure S2 (a) TEM image of MQDs, the inset was the particle size statistics of MQDs
and (b) AFM image of MQDs.

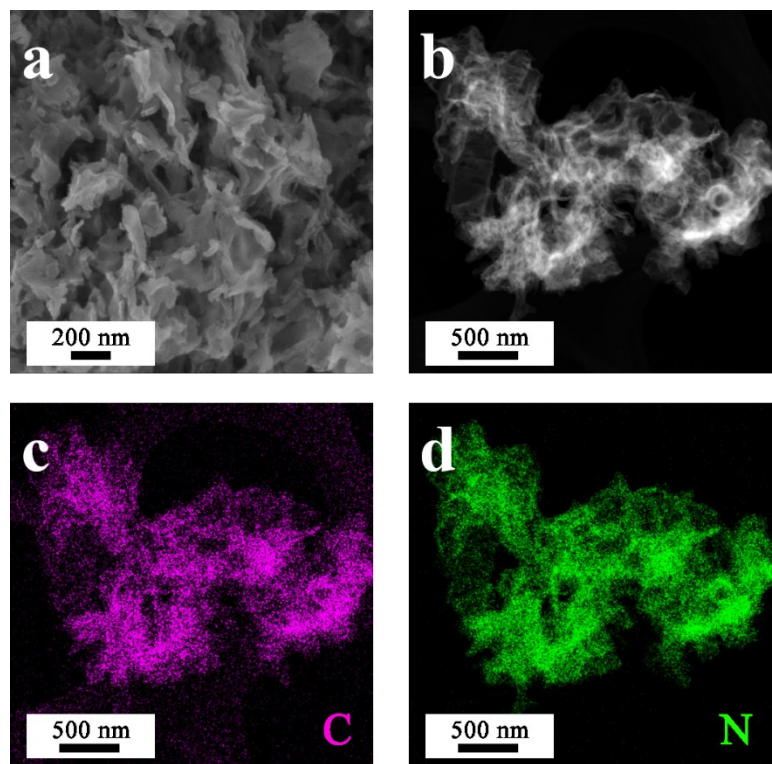


Figure S3 (a) SEM image, (b) HAADF image and (c, d) corresponding elemental mappings of $\text{g-C}_3\text{N}_4$.

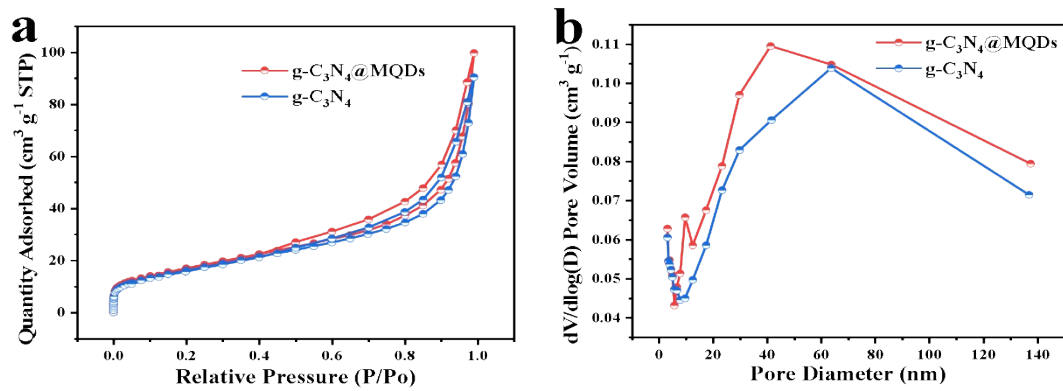


Figure S4 (a) N_2 adsorption-desorption curve and (b) pore size distribution curve of $\text{g-C}_3\text{N}_4$ @MQDs and $\text{g-C}_3\text{N}_4$.



Figure S5 Optical images of (a) Celgard, (b) GC and (c) GMC separator.

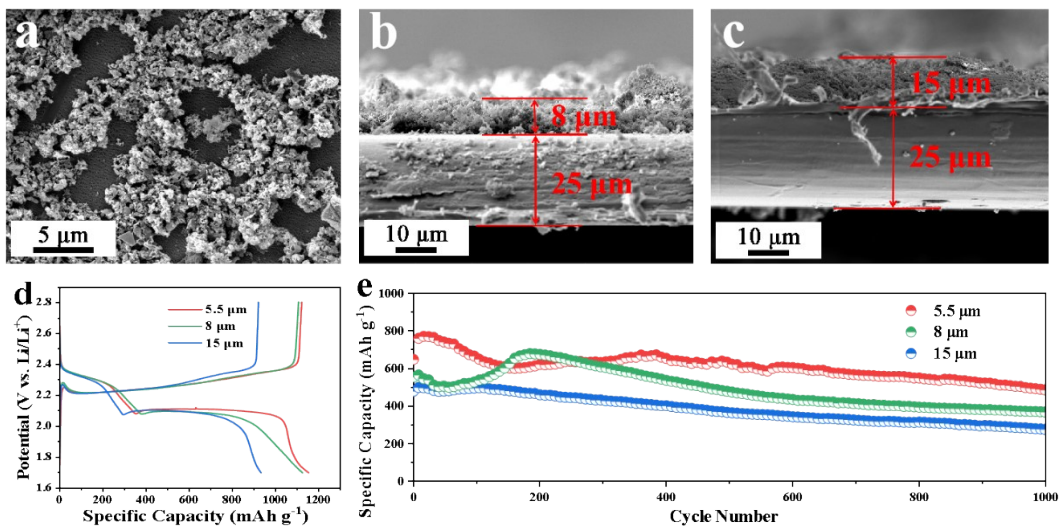


Figure S6 (a) SEM image of GMC separator with a loading of 0.05 mg cm^{-2} . Cross section SEM image of GMC separator with a loading of (b) 0.2 mg cm^{-2} and (c) 0.3 mg cm^{-2} , the corresponding thickness of the modified layer is $8 \mu\text{m}$ and $15 \mu\text{m}$. (d) Galvanostatic charge/discharge curves of Li-S cells assembled by GMC separator with different thickness at 0.2 C . (e) Cycling performance of Li-S cells assembled by GMC separator with different thickness at 2 C .

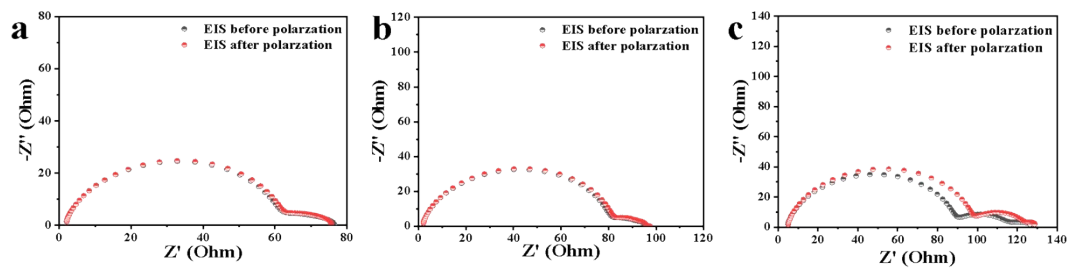


Figure S7 The EIS curve before and after polarization of Li//Li symmetrical batteries

with (a) GMC, (b) GC and (c) Celgard separator.

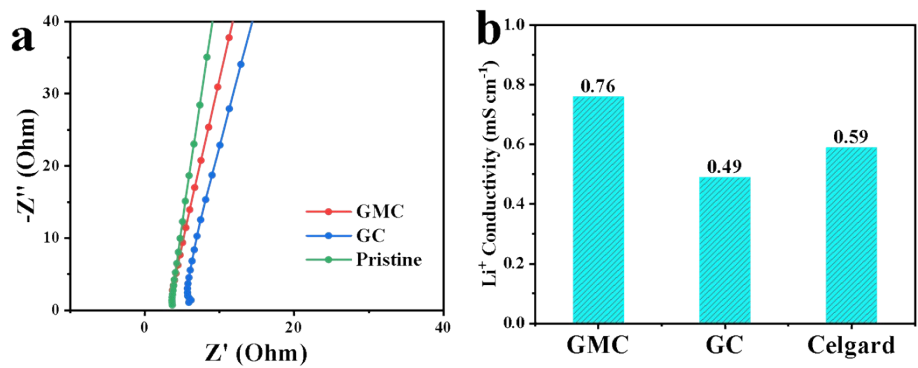


Figure S8 (a) Electrochemical impedance spectra and (b) corresponding ionic conductivities of various separators.

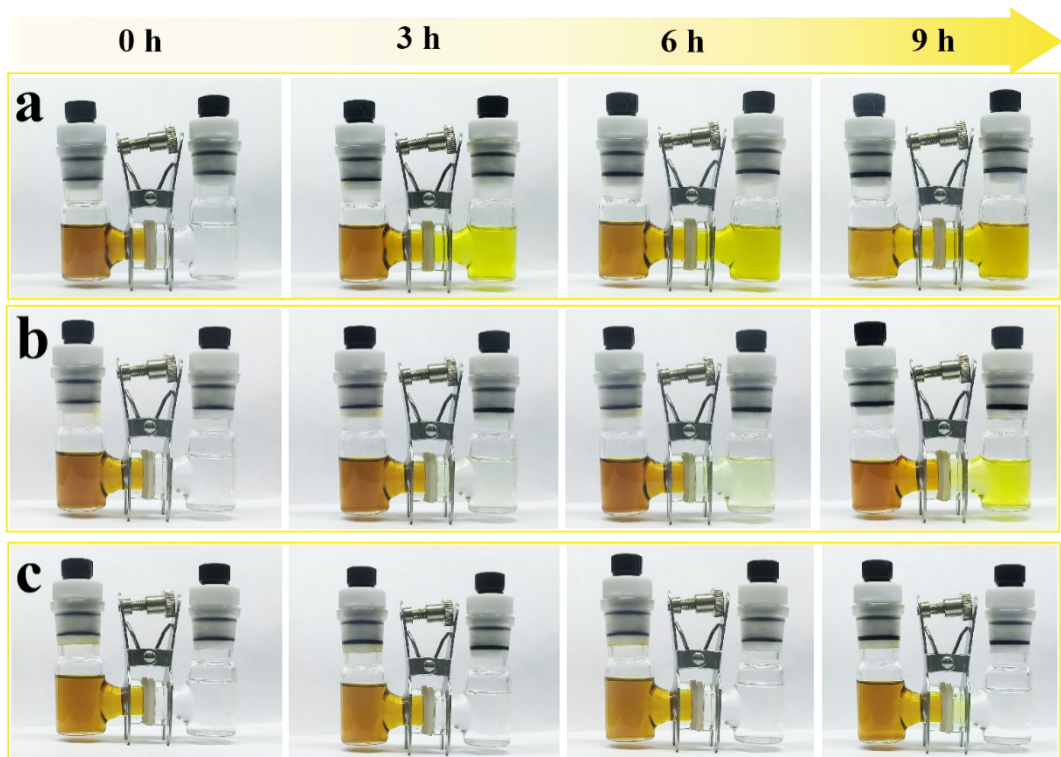


Figure S9 Visual shuttle experiment using different separators: (a) Pristine Celgard, (b) GC and (c) GMC.

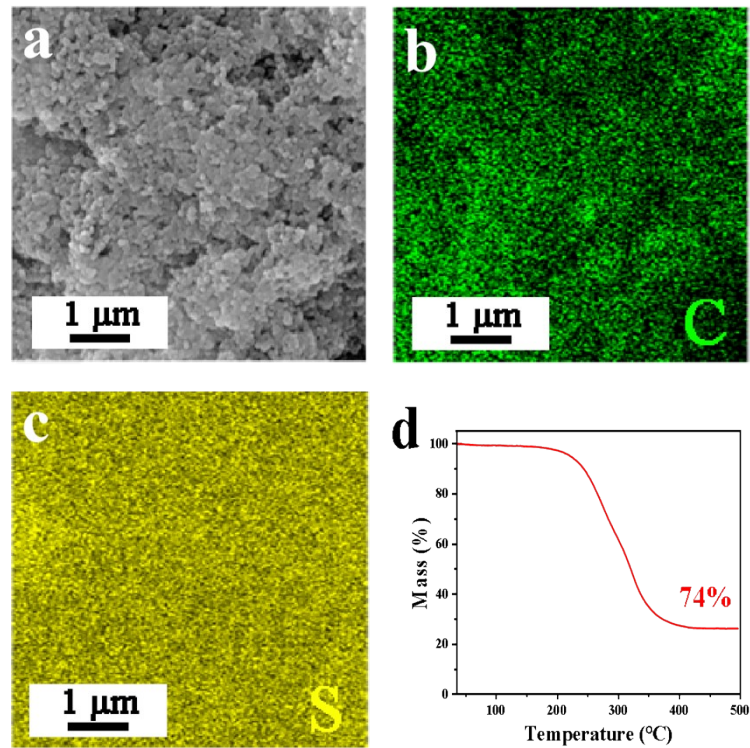


Figure S10 (a) SEM image of KJC/S electrode and corresponding mappings of (b) C, (c) S. (d) TGA curve of KJC/S.

Table S1 The comparisons of the comprehensive electrochemical performance of Li-S cells with various separators.

Separator	Max capacity (mAh g ⁻¹)	Rate capacity (mAh g ⁻¹)	Cycling performance			Ref.
			Rate	Cycle number	Fading	
CG-CFG@Mo ₂ C	1632 (0.1 C)	755 (3 C)	0.5 C	400	0.068%	S1
SrF ₂ -G	1311 (0.1 C)	878 (3 C)	1.0 C	350	0.050%	S2
MoCo@CHS ₃ -PP	1022 (0.2 C)	575 (3 C)	1.0 C	600	0.066%	S3
ZnS/NCNS-PP	1480 (0.2 C)	930 (2 C)	2.0 C	800	0.039%	S4
NbN@NG	1284 (0.2 C)	819 (4C)	2.0 C	500	0.036%	S5
MnO ₂ @PE	1345 (0.1 C)	689 (3 C)	0.5 C	500	0.059%	S6
STO-W/S	1242 (0.1 C)	492 (2 C)	1.0 C	500	0.067%	S7
Mo ₂ N@NG	1309 (0.2 C)	860 (4 C)	2.0 C	800	0.039%	S8
ReS ₂ @NG/PP	1350 (0.2 C)	810 (2 C)	2.0 C	80	0.064%	S9
CNF-VS ₄	1135 (0.2 C)	780 (2 C)	5.0 C	1000	0.050%	S10
g-C ₃ N ₄ /PP	990 (0.2 C)	400 (5 C)	0.2 C	200	0.081%	S11
g-C ₃ N ₄ /glass fiber	1166 (0.5 C)	732 (1 C)	0.5 C	400	0.070%	S12
Co-TCN@PP	1304 (0.1 C)	863 (2 C)	2.0 C	400	0.070%	S13
CoS@g-C ₃ N ₄	1290 (0.2 C)	690 (2 C)	1.0 C	500	0.030%	S14
g-C ₃ N ₄ /CNT@PP	1200 (0.1 C)	755 (2 C)	1.0 C	500	0.030%	S15
Porous MXene/PP	1282 (0.1 C)	677 (2 C)	1.0 C	500	0.070%	S16
Ti ₃ C ₂ T _x /Ni-Co@PP	1260 (0.2 C)	910 (1 C)	1.0 C	500	0.050%	S17
TiN@C/G	1490 (0.1 C)	647 (2 C)	1.0 C	600	0.047%	S18
MPF13-550/PP	1235 (0.1 C)	593 (2 C)	2.0 C	200	0.120%	S19
g-C ₃ N ₄ @MQDs	1433 (0.1 C)	532 (4 C)	2.0 C	1000	0.024%	This work

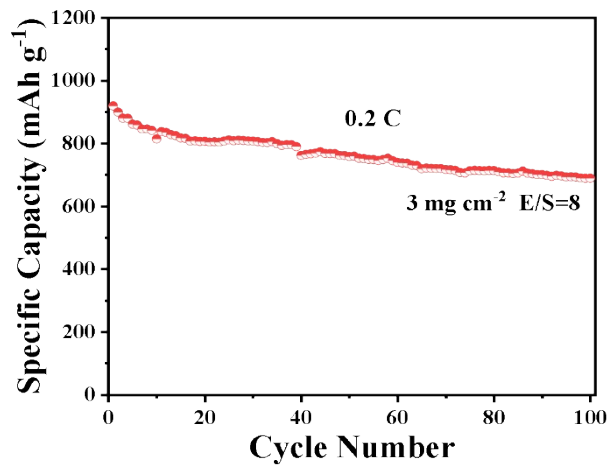


Figure S11 Cycling performance of Li-S cells assembled by GMC separator at a high sulfur loading of 3 mg cm^{-2} .

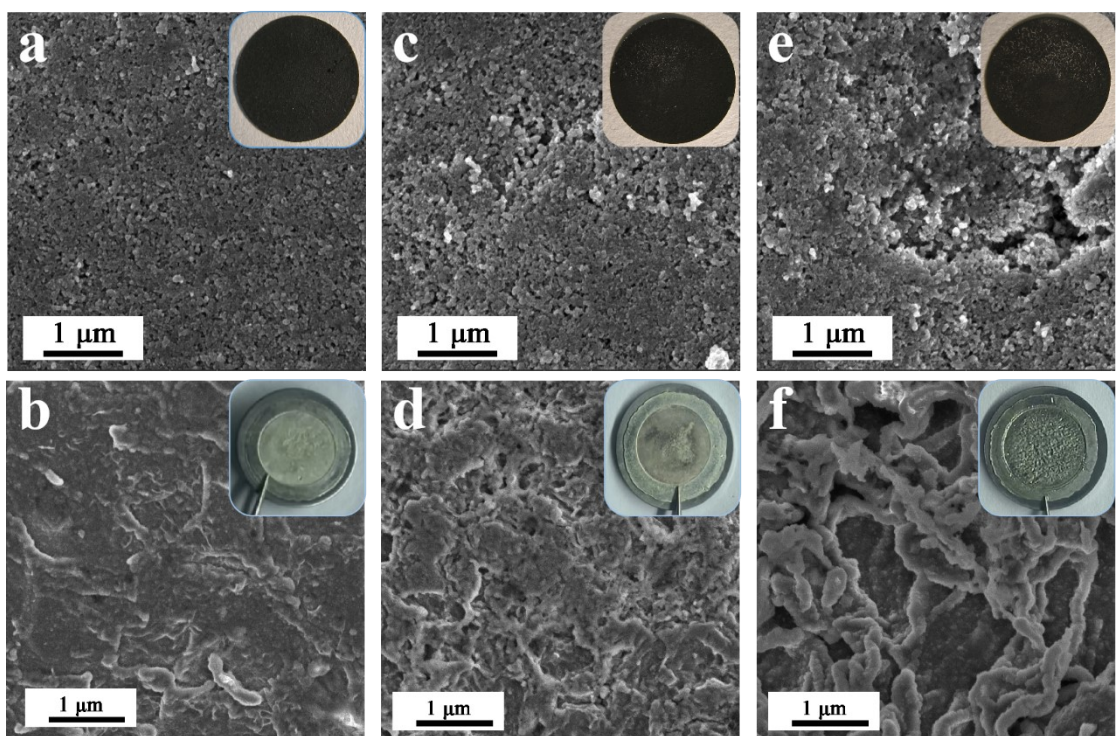


Figure S12 SEM images of the positive and negative electrodes of Li-S batteries with different separators after cycling: (a, b) GMC, (c, d) GC and (e, f) pristine Celgard. The insets were the corresponding optical picture.

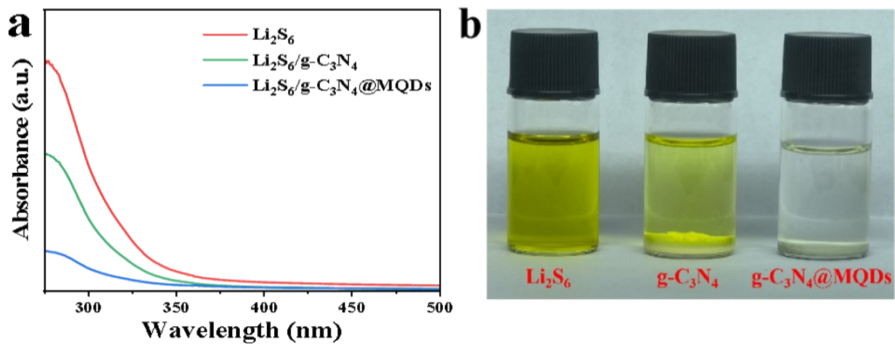


Figure S13 (a) Uv-vis spectra and (b) digital photos of Li_2S_6 solution and Li_2S_6 solution after the addition of $\text{g-C}_3\text{N}_4$ and $\text{g-C}_3\text{N}_4@\text{MQDs}$.

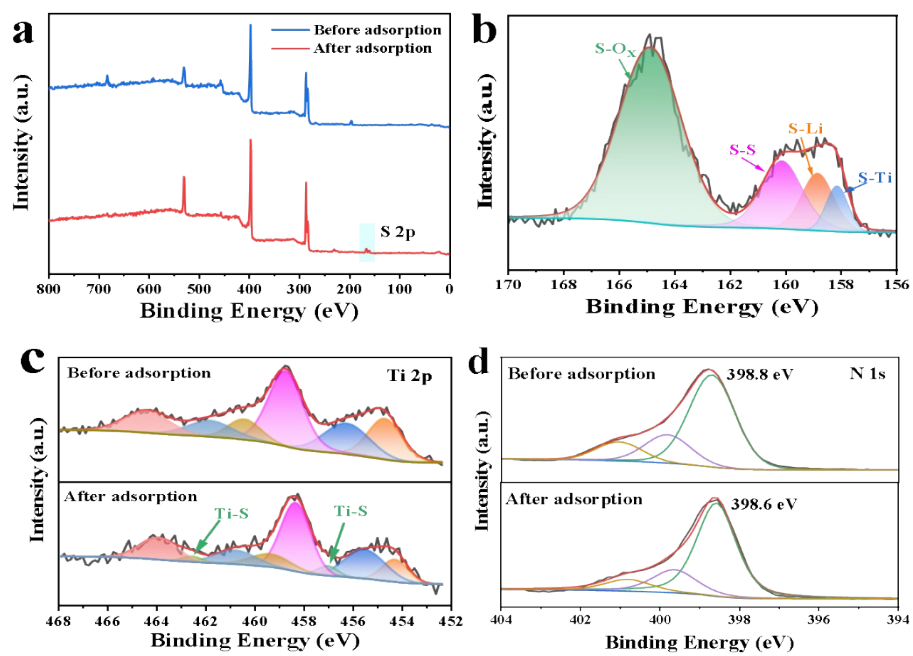


Figure S14 (a) XPS full spectra and high-resolution spectra of (b) S 2p, (c) Ti 2p and (d) N 1s before and after the adsorption of Li_2S_6 .

References

- S1. Y. C. Mo, J. S. Lin, S. S. Li and J. Yu, Chemical Engineering Journal, 2022, 433, 134306.
- S2. W. T. Jing, J. H. Zu, K. Y. Zou, X. Dai, Y. Y. Song, J. Q. Han, J. J. Sun, Q. Tan, Y. Z. Chen and Y. N. Liu, Journal of Materials Chemistry A, 2022, 10, 4833-4844.
- S3. Y. L. Wang, F. Y. Ma, G. S. Wang, X. B. Wu, Q. H. Meng and X. J. Zou, Journal of Alloys and Compounds, 2022, 923, 166445.
- S4. Z. Li, F. Zhang, L. Tang, Y. Tao, H. Chen, X. M. Pu, Q. J. Xu, H. M. Liu, Y. G. Wang and Y. Y. Xia, Chemical Engineering Journal, 2020, 390, 124653.
- S5. F. Ma, X. Zhang, K. Sriniva, D. Liu, Z. Zhang, X. Chen, W. Zhang, Q. Wu and Y. Chen, Journal of Materials Chemistry A, 2022, 10, 8578-8590.
- S6. X. Song, G. Chen, S. Wang, Y. Huang, Z. Jiang, L. X. Ding and H. Wang, ACS Applied Materials & Interfaces, 2018, 10, 31, 26274-26282.
- S7. Z. D. Huang, M. Yang, J. Qi, P. Zhang, L. Lei, Q. C. Du, L. Bai, H. Fu, X. Yang, R. Liu, T. Masesed, H. Zhang, Y. W. Ma, Chemical Engineering Journal, 2020, 387, 124080.
- S8. Ma, K. Srinivas, X. Zhang, Z. Zhang, Y. Wu, D. Liu, W. Zhang, Q. Wu and Y. Chen, Advanced Functional Materials, 2022, 32, 2206113.
- S9. N. Wei, J. Cai, R. Wang, M. Wang, Wei. Lv, H. Ci, J. Sun, Z. Liu, Nano Energy, 2019, 66, 104190.
- S10. Y. Zhang, G. Xu, Q. Kang, L. Zhan, W. Tang, Y. Yu, K. Shen, H. Wang, X. Chu, J. Wang, S. Zhao, Y. Wang, L. Ling and S. Yang, Journal of Materials Chemistry A,

2019,7, 16812-16820.

- S11. Y. G. Huangfu, T. T. Zheng, K. Zhang, X. J. She, H. Xu, Z. Fang and K. Y. Xie, *Electrochimica Acta*, 2018, 272, 60-67.
- S12. C. Y. Fan, H. Y. Yuan, H. H. Li, H. F. Wang, W. L. Li, H. Z. Sun, X. L. Wu and J. P. Zhang, *ACS Applied Materials & Interfaces*, 2016, 8, 16108-16115.
- S13. Z. Fan, M. Zhu, S. Deng, Y. Chen, Y. Zhao, M. Qin, G. Ma, J. Wu and X. Xin, *Nanoscale Advances*, 2022, DOI: 10.1039/D2NA00645F.
- S14. X. Y. Liu, S. X. Wang, H. N. Duan, Y. F. Deng and G. H. Chen, *Journal of Colloid and Interface Science*, 2022, 608, 470-481.
- S15. X. L. Wang, G. R. Li, M. J. Li, R. P. Liu, H. B. Li, T. Y. Li, M. Z. Sun, Y. R. Deng, M. Feng and Z. W. Chen, *Journal of Energy Chemistry*, 2021, 53, 234-240.
- S16. D. B. Xiong, S. Z. Huang, D. L. Fang, D. Yan, G. J. Li, Y. P. Yan, S. Chen, Y. L. Liu, X. L. Li, Y. Von Lim, Y. Wang, B. B. Tian, Y. M. Shi and H. Y. Yang, *Small*, 2021, 17.
- S17. Y. L. Ren, Q. X. Zhai, B. Wang, L. B. Hu, Y. J. Ma, Y. M. Dai, S. C. Tang and X. K. Meng, *Chemical Engineering Journal*, 2022, 439.
- S18. Y. P. Fan, K. G. Liu, A. Ali, X. F. Chen and P. K. Shen, *Electrochimica Acta*, 2021, 384.
- S19. L. W. Lin, M. Qi, Z. T. Bai, S. X. Yan, Z. Y. Sui, B. H. Han and Y. W. Liu, *Applied Surface Science*, 2021, 555.